

Electrosorption of Tetraethylene Glycol Monododecyl Ether at the Polarized Nitrobenzene–Water Interface

Takashi KAKIUCHI, Taketoshi USUI, and Mitsugi SENDA*

Department of Agricultural Chemistry, Faculty of Agriculture, Kyoto University,
Sakyo-ku, Kyoto 606

(Received March 12, 1990)

The adsorption of tetraethylene glycol monododecyl ether, C12E4, has been studied by measuring the electrocapillary curves at the polarized interface between the nitrobenzene solution of 0.1 mol dm⁻³ tetrapentylammonium tetraphenylborate and the aqueous solution of 0.05 mol dm⁻³ lithium chloride. C12E4 adsorbed at the interface over the entire polarized potential range of 250 mV. Although C12E4 itself is a neutral molecule, its surface activity was greatly affected by changing the potential drop across the interface; an increase in the potential of the aqueous phase with respect to the potential in the nitrobenzene phase markedly enhanced the adsorption. The complex formation between the adsorbed C12E4 molecules and Li⁺ ions in the aqueous side of the interface was shown to play a decisive role in determining the dependence of adsorption on the electrical potential difference across the interface. A proposed model for complex formation at the interface based on the Gouy–Chapman double-layer theory well-explained the observed trend in the adsorption Gibbs energy when the potential drop across the interface was changed.

The effect of the electrical potential difference across the interface on the surface activity of surfactants is of great importance not only in understanding various surface phenomena, but also in the field of practical applications of surfactants, since its surface activity can be controlled by regulating the electrical state of the interface. Guastalla first found the fact that the adsorption of hexadecyltrimethylammonium ion at the nitrobenzene–water interface was very much influenced by the applied potential,¹⁾ and called this phenomenon “electroadsorption”, since, according to him, no effect was observed when no long-chain electrolytes were dissolved in both phases. Later, Watanabe et al. studied the effect of an applied potential on the surface activity of various surfactants at the methyl isobutyl ketone–water interface by applying the concept of electrocapillarity.²⁾ As exemplified by our previous studies of the adsorption of hexadecyltrimethylammonium ion at the polarized nitrobenzene–water interface,^{3,4)} the effect of the electrical state of the interface on the surface activity of surfactants at oil–water interfaces is best studied by using an ideally polarized oil–water interface, where the electrocapillarity can be studied under the well-defined electrical state of the interface.⁵⁾ Since the term “electroadsorption” has been used almost exclusively, in distinction from “electrocapillarity”, to indicate the adsorption of ionic components at the oil–water interface under the passage of significant electric current,^{6,7)} we shall use in this paper the term “electrosorption”, which has been used in studies of the adsorption on electrodes,⁸⁾ as a concise expression for designating explicitly the adsorption phenomena under the influence of electrical variables. The effect of the electrical potential difference at the interface is not limited to the case of ionic surfactants. The adsorption of neutral surfactants is also expected to be

affected by the electrical state of the interface. First, the difference in the polarizability as well as in the dipole moment between the adsorbate and solvent molecules gives rise to a difference in the electrical energy of the interface, as is well-known in the adsorption of organic compounds on electrodes.⁹⁾ Second, nonionic surfactants having an oxyethylene group as a hydrophilic group are capable of forming complexes with ions and behave as if they are charged species. The latter properties of the nonionic surfactants have been utilized for solvent extraction^{10–12)} and selective ion transport in biological membrane processes¹³⁾ as well as the selective detection of ions in ion-selective electrode.¹⁴⁾ Recently, in a study of ion transfer across an nitrobenzene–water interface facilitated by Triton X's, Yoshida and Kihara¹⁵⁾ suggested using a dropping electrolyte solution electrode that the adsorption of Triton X's would be dependent on the applied voltage across the interface. The purpose of the present study was to extend our previous studies concerning the electrosorption of ionic surfactants at the polarized oil–water interface to nonionic surfactants for characterizing their adsorption properties thermodynamically under a well-defined electrical state of the interface. This paper deals with the electrosorption of tetraethylene glycol monododecyl ether, C12E4, at the polarized interface between the nitrobenzene solution of tetrapentylammonium tetraphenylborate, TPnATPB, and an aqueous solution of lithium chloride studied by measuring equilibrium electrocapillary curves.¹⁶⁾

Experimental

The interfacial tension was measured at 25±0.05 °C using a computer-aided pendant drop method.¹⁷⁾ Details of this method were described elsewhere.¹⁷⁾ Nitrobenzene solutions of TPnATPB containing various amounts of C12E4 were shaken with an aqueous solution of lithium chloride

overnight at 25 °C for ensuring partition equilibrium. In the measurement, a drop of a nitrobenzene solution was formed at the tip of a glass tubing immersed in the aqueous phase. After the formation of a drop, the drop image was recorded at a fixed applied potential, which was stepwise increased by 20 mV from negative to positive every 30 sec. The potential drop across the interface was controlled with a laboratory-made four-electrode potentiostat.¹⁷⁾ The polarizability of the interface was monitored through linear potential sweep voltammetry recorded prior to an interfacial tension measurement. The residual ohmic potential drop due to an uncompensated solution resistance was compensated for by using a positive feedback method. The amount of the feedback voltage was adjusted to be just below the point of oscillation of the system.

High-purity C12E4 was obtained from Nikko Chemicals (Japan) and used without further purification. Nitrobenzene was first distilled under reduced pressure and then treated with active alumina. Water was treated with an NANOpure II system (Barnstead, MA., USA) and then distilled from potassium permanganate solution. TPnATPB was prepared as described elsewhere.³⁾ An aqueous solution of tetrapentylammonium chloride, TPnACl, was saturated with silver chloride. The TPnACl concentration was determined by a potentiometric titration of chloride ion. Lithium chloride monohydrate (a Merck's Spurapur grade) was used without further purification. The concentration of C12E4 in the aqueous phase in partition equilibrium with a nitrobenzene solution containing C12E4 was determined polarographically using the suppression of the polarographic maximum on a oxygen-reduction wave. The concentration of nitrobenzene in the aqueous phase was also measured polarographically from the limiting current of a nitrobenzene reduction wave.

Results

The electrochemical cell used for the electrocapillary curve measurements is represented by:

I	II	III	IV	V	VI	VII
Ag	AgCl	0.02 M ^{a)} TPnACl	0.1 M TPnATPB + x mM C12E4	0.05 M LiCl	AgCl	Ag
		(water)	(nitrobenzene)	(water)		

The interface between IV and V is the polarized interface and the interface between III and IV is the nonpolarized interface, which served as part of the reference electrode reversible to TPnA⁺ ion in the phase IV. The potential of the right-hand side terminal of the cell was measured with respect to the potential of the left and is hereafter referred to as E . The linear potential sweep voltammogram for this cell at $x=1$, 10, and 100 are shown in Fig. 1, after subtracting the voltammogram for $x=0$. The polarized range became narrower with increasing concentration of C12E4. The analysis of the current vs. potential curves¹⁸⁾ indicated that this increase in the current was due to the facilitated transfer of Li⁺ ions

^{a)} 1 M = 1 mol dm⁻³.

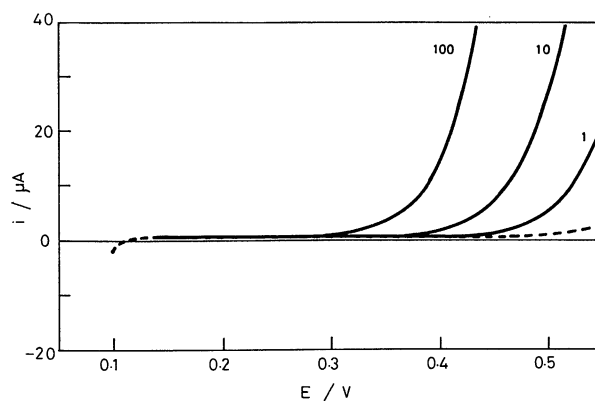


Fig. 1. Linear potential sweep voltammograms in the presence (—) and in the absence (---) of C12E4 in the nitrobenzene phase; scan rate is 20 mV s⁻¹ and the area of the interface is 0.279 cm². The concentration of C12E4 is indicated by each line in mmol dm⁻³.

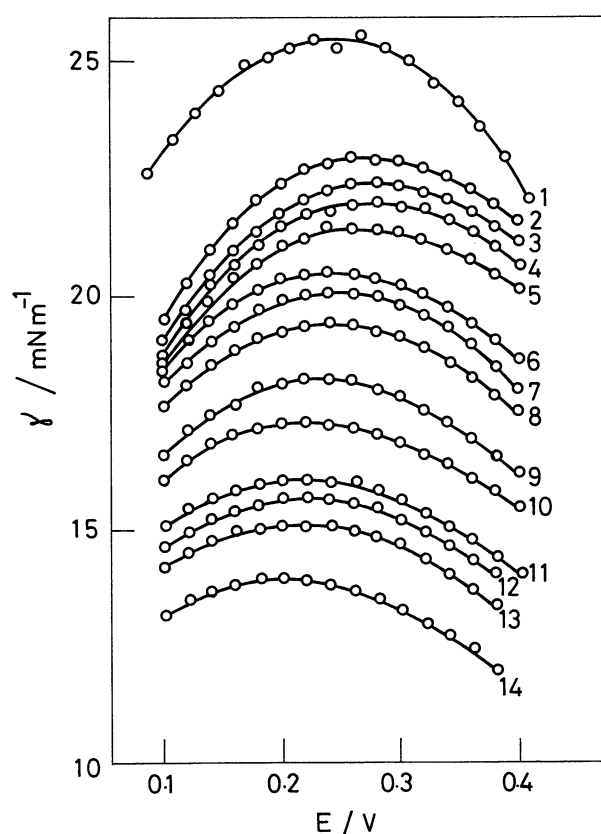


Fig. 2. Electrocapillary curves at 25 °C for the interface between the nitrobenzene solution of 0.1 mol dm⁻³ TPnATPB and the aqueous solution of 0.05 mol dm⁻³ LiCl in the presence of x mmol dm⁻³ C12E4: $x=0$ (1), 1(2), 2(3), 5(4), 7(5), 10(6), 15(7), 20(8), 30(9), 40(10), 50(11), 70(12), 80(13), and 100(14).

from the aqueous phase to the nitrobenzene phase. The interfacial tension was measured at 20 mV intervals of the applied voltage in the polarized range for 13 concentrations of C12E4 between $x=1$ and 100.

The electrocapillary curves are shown in Fig. 2. The interfacial tension was lowered with the C12E4 concentration over the entire polarized range, indicating the adsorption of C12E4 at the interface. The monotonous decrease in the interfacial tension with the C12E4 concentration without a break point indicates the absence of appreciable micelle formation in the nitrobenzene phase up to 100 mmol dm⁻³ of C12E4.

From the general electrocapillary equation for the polarized oil-water interface,¹⁹⁾ the derivative of the interfacial tension, γ , with respect to the chemical potential of C12E4, μ_{C12E4} , at constant temperature, pressure, and chemical potentials of the components except C12E4 is expressed in this case as

$$-\left(\frac{\partial \gamma}{\partial \mu_{\text{C12E4}}}\right)_{T,P,E,\mu_{i \neq \text{C12E4}}} = \Gamma_{\text{C12E4}} - J x_{\text{C12E4}}^{\text{NB}} - K x_{\text{C12E4}}^{\text{W}}, \quad (1)$$

$$J = \frac{\Gamma_{\text{W}} x_{\text{NB}}^{\text{W}} - \Gamma_{\text{NB}} x_{\text{W}}^{\text{W}}}{x_{\text{NB}}^{\text{W}} x_{\text{W}}^{\text{NB}} - x_{\text{NB}}^{\text{NB}} x_{\text{W}}^{\text{W}}},$$

and

$$K = \frac{\Gamma_{\text{W}} x_{\text{W}}^{\text{NB}} - \Gamma_{\text{W}} x_{\text{NB}}^{\text{NB}}}{x_{\text{NB}}^{\text{W}} x_{\text{W}}^{\text{NB}} - x_{\text{NB}}^{\text{NB}} x_{\text{W}}^{\text{W}}},$$

where Γ_i is the surface excess of species i , ($i = \text{C12E4}$, W, or NB; W and NB stand for water and nitrobenzene), and x_i^α is the mole fraction of a component i in phase α , (α denotes aqueous or nitrobenzene phase as W or NB). To estimate the contribution of the second and third terms on the right-hand side of the Eq. 1 to the left, we measured the concentrations of C12E4 and nitrobenzene in the aqueous phase as follows. 10 ml of a nitrobenzene solution containing 500 mmol dm⁻³ C12E4 in addition to 0.1 mol dm⁻³ TPnATPB was shaken with a 100 ml aqueous solution of 0.05 mol dm⁻³ LiCl. The equilibrium concentration of C12E4 in the aqueous phase was found to be below the detection limit of this method, 1 $\mu\text{mol dm}^{-3}$, which in the present case was bound by the presence of nitrobenzene distributed in the aqueous phase; the partition coefficient of C12E4 between nitrobenzene and water was estimated to be at least larger than 98. The nitrobenzene concentration in the aqueous solution was found to be 15 ± 1 mmol dm⁻³. This value agrees well with a literature value of 16.4 mmol dm⁻³²⁰⁾ for the partition equilibrium without supporting electrolytes. On the other hand, the concentration of water in water-saturated nitrobenzene is 0.00295 at 25 °C in mole fraction scale.²⁰⁾ Therefore, the terms $x_{\text{C12E4}}^{\text{W}}$, x_{NB}^{W} , and x_{W}^{NB} in Eq. 1 can safely be ignored and Eq. 1 is reduced to

$$-\left(\frac{\partial \gamma}{\partial \mu_{\text{C12E4}}}\right)_{T,P,E,\mu_{i \neq \text{C12E4}}} = \Gamma_{\text{C12E4}} - \frac{x_{\text{C12E4}}^{\text{NB}}}{x_{\text{NB}}^{\text{NB}}} \Gamma_{\text{NB}}. \quad (2)$$

Furthermore, the second term on the r.h.s. of Eq. 2 is negligibly small by two reasons; first, $x_{\text{C12E4}}^{\text{NB}}/x_{\text{NB}}^{\text{NB}}$ is negligibly small, since this term is in the present case not greater than 0.015, and, second, Γ_{NB} would not significantly be larger than Γ_{C12E4} . Hence, the derivative in Eq. 2 directly gives the value of Γ_{C12E4} and can be seen as being the adsolute amount of adsorbed C12E4 at the interface. In the following analysis, the activity of C12E4 in the nitrobenzene phase was equated to its concentration, $c_{\text{C12E4}}^{\text{NB}}$.

The Γ_{C12E4} values were obtained from the numerical differentiation of γ vs. $\log c_{\text{C12E4}}^{\text{NB}}$ curves at constant E using a B-spline function and are plotted in Fig. 3 as a function of E at several $c_{\text{C12E4}}^{\text{NB}}$ values. The Γ_{C12E4} value increased with a positive increase in E . The adsorption isotherms at $E = 0.12, 0.18$ and 0.25 V shown in Fig. 4 were fitted to the Langmuir isotherm:

$$Bc = \frac{\theta}{(1 - \theta)}, \quad (3)$$

where B is the adsorption coefficient, $\theta = \Gamma_{\text{C12E4}}/\Gamma_{\text{C12E4}}^{\text{m}}$ and $\Gamma_{\text{C12E4}}^{\text{m}}$ is the maximum adsorption. From the intercept and the slope of the plots in Fig. 5, the values

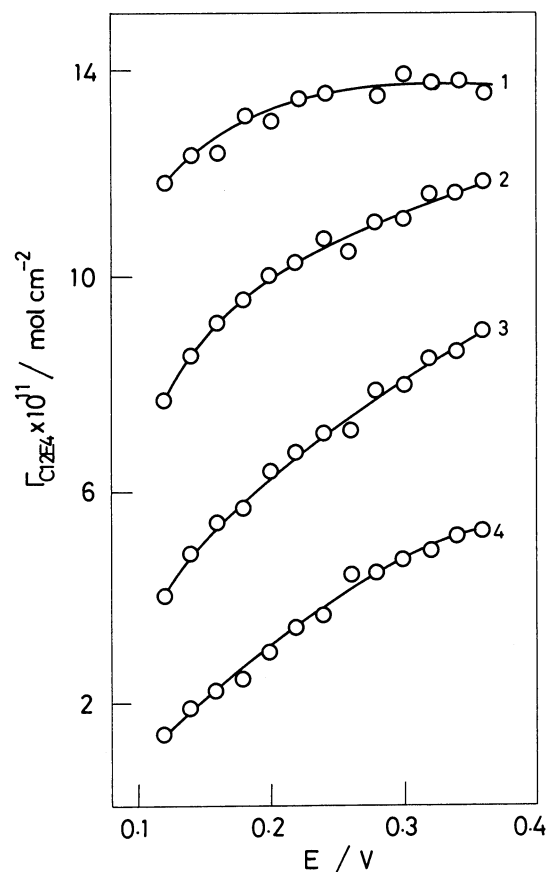


Fig. 3. Dependence of the adsorbed amount of C12E4, Γ_{C12E4} , on E at the concentration of C12E4 in the nitrobenzene phase being, $c_{\text{C12E4}}^{\text{NB}} = 50(1), 20(2), 10(3),$ and $5(4)$ mmol dm⁻³.

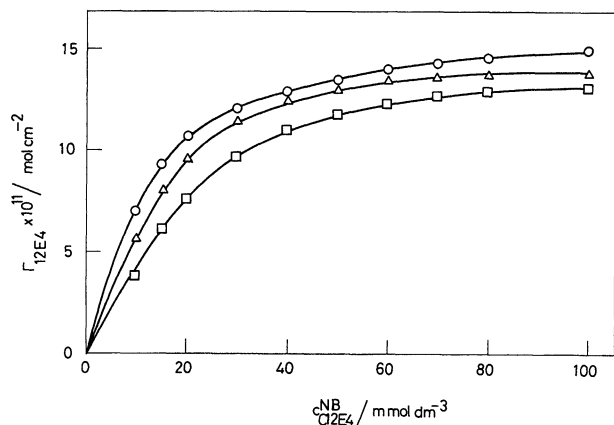


Fig. 4. Adsorption isotherms of C12E4 at $E=0.120$ (□), 0.180 (Δ), and 0.240 (○) V.

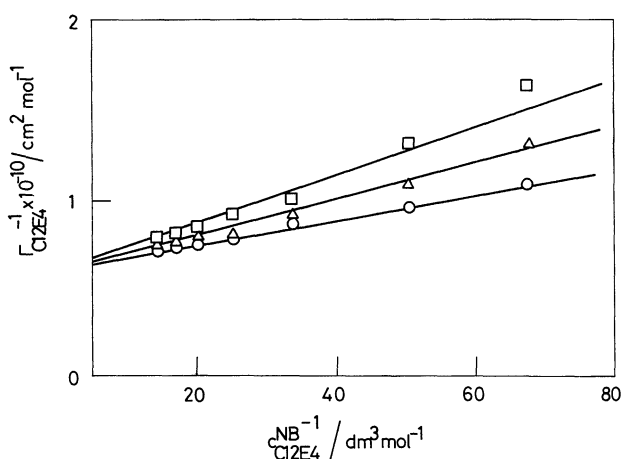


Fig. 5. Plot of $1/\Gamma_{\text{C12E4}}$ vs. $1/c_{\text{C12E4}}^{\text{NB}}$ at $E=0.120$ (□), 0.180 (Δ), and 0.240 (○) V to test the Langmuir isotherm.

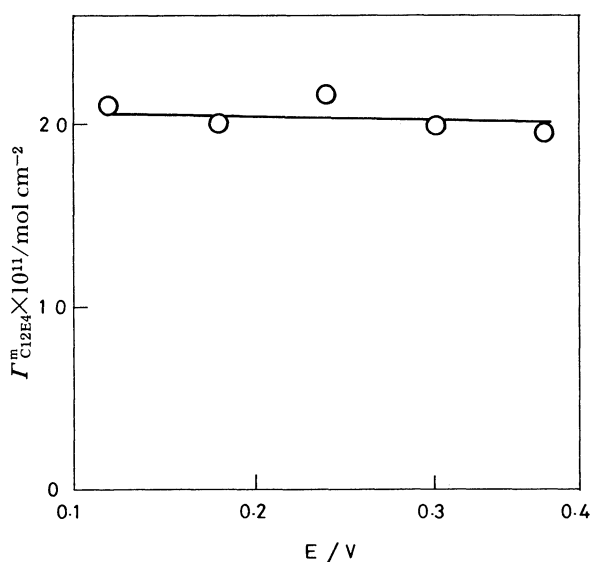


Fig. 6. Dependence of the maximum adsorption of C12E4, $\Gamma_{\text{C12E4}}^{\text{m}}$, on E .

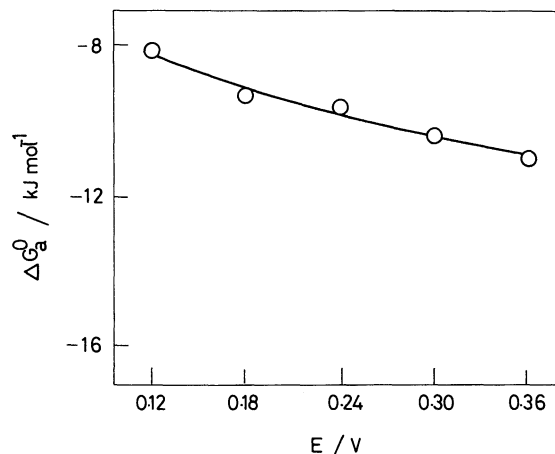


Fig. 7. Dependence of the standard adsorption Gibbs energy, ΔG_a^o , on E .

for $\Gamma_{\text{C12E4}}^{\text{m}}$ and B were estimated and the latter quantity was converted to the standard adsorption Gibbs energy, ΔG_a^o , whose standard states were 1 mol dm^{-3} for the aqueous phase and $\theta=1$ for the interface, both of them referring to infinite dilution. Figure 6 shows that $\Gamma_{\text{C12E4}}^{\text{m}}$ is virtually independent of E , while ΔG_a^o decreases with increasing E (Fig. 7).

Discussion

The surface activity of C12E4 at the nitrobenzene-water interface shows a remarkable dependence on the potential drop across the interface (Fig. 3), although the C12E4 molecule, itself, bears no net charge. The constancy of $\Gamma_{\text{C12E4}}^{\text{m}}$ with respect to E (Fig. 6) suggests that the change in E does not induce any change in the orientation of the adsorbed C12E4 molecules nor the formation of a multilayer; the effect of E is primarily on ΔG_a^o . In the case of the adsorption of neutral organic compounds on electrodes, the adsorption does depend on the electrical state of the interface.⁹⁾ This is due the difference in the energies of the portion of the interface covered and uncovered by the adsorbed organic molecules.²¹⁾ In fact, the adsorption properties of most of the organic compounds at electrode-solution interfaces conform to the two parallel condenser model based on the above reasoning proposed by Frumkin.²²⁾ This model predicts that ΔG_a^o is a quadratic function of E and decreases as E away from the potential of maximum adsorption, provided that the capacitance value at $\theta=1$ is larger than at $\theta=0$. Indeed, the ΔG_a^o vs. E curve in Fig. 7 is of slightly concave form and may be seen as a quadratic function. In fact, the adsorption of C12E4²³⁾ and other homologous surfactants^{24,25)} at the electrified interface between mercury and water can essentially be interpreted in terms of this model.

However, this model does not seem to be appropriate to give a satisfactory explanation of the observed

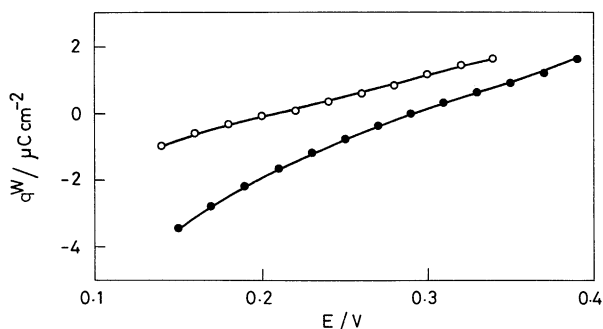


Fig. 8a. Dependence of excess surface charge density, q^w , on E at $c_{\text{C12E4}}^{\text{NB}}=0$ (●) and 80 (○) mmol dm⁻³.

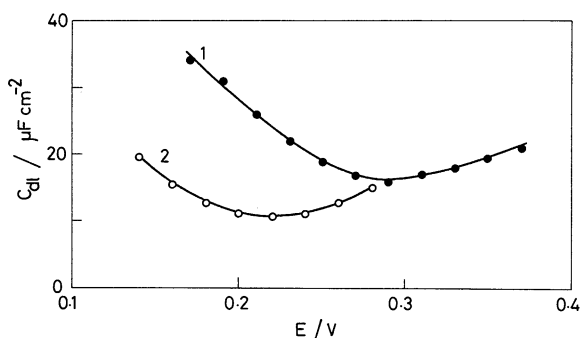
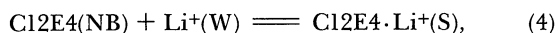


Fig. 8b. Dependence of the double layer capacitance, C_{dl} , on E at $c_{\text{C12E4}}^{\text{NB}}=0$ (●) and 80 (○) mmol dm⁻³.

adsorption behavior of C12E4 at the nitrobenzene–water interface. Figures 8a and 8b show the excess charge density in the aqueous phase, q^w , and the double-layer capacitance, C_{dl} , when $x=0$ and $x=80$, evaluated from the first and second derivative of the corresponding electrocapillary curves with respect to E . As can be seen in Fig. 8b, the difference in the C_{dl} values becomes smaller and the two curves merge together in the region where the adsorption becomes maximum in the polarized range. On the other hand, the two parallel-plate condenser model implies that the difference in the two C_{dl} values is greatest around E_m ; in fact, this is the case in the C12E4 adsorption on the mercury electrode.²⁴⁾

An alternative interpretation for the observed sensitivity of the C12E4 surface activity against the change in E is the complexation of C12E4 at the interface with counterions in the aqueous side of the interface:



where S denotes the interface. The facilitated transfer of Li⁺ ions seen at the positive and of the polarized (Fig. 1) suggests the occurrence of this complex formation, even in a less positive range of E . The stability constant, K , for the above reaction is defined by

$$K = \frac{\Gamma_{\text{C12E4} \cdot \text{Li}}}{\Gamma_{\text{C12E4}} s_{\text{Li}}^w}, \quad (5)$$

where s_{Li}^w is the surface concentration of Li⁺ ion, and Γ_{C12E4} and $\Gamma_{\text{C12E4} \cdot \text{Li}}$ are the adsorbed amounts of the free C12E4 and the complex, C12E4·Li⁺. Then, the total surface excess of C12E4 obtainable experimentally is the sum¹⁹⁾

$$\Gamma_{\text{total}} = \Gamma_{\text{C12E4}} + \Gamma_{\text{C12E4} \cdot \text{Li}}, \quad (6)$$

and the corresponding $\Delta G_{\text{a,total}}^0$, which is evaluated from the limiting slope of an adsorption isotherm when $C_{\text{C12E4}}^{\text{NB}}$ approaches zero, can be expressed as (See Appendix)

$$\Delta G_{\text{a,total}}^0 = \Delta G_{\text{a,f}}^0 - RT \ln(1 + K s_{\text{Li}}^w), \quad (7)$$

where $\Delta G_{\text{a,f}}^0$ is the standard adsorption Gibbs energy in the absence of surface complexation.

s_{Li}^w is, in general, a function of the electrical state of the interface. On estimating the s_{Li}^w values, we assumed that complexation took place at the outer Helmholtz plane in the aqueous side, OHP^w, and s_{Li}^w was given by the Gouy-Chapman theory.^{26,27)} This simplified treatment may be justified, since the double-layer structure at the polarized nitrobenzene–water interface in the absence of specific adsorption can be well described by this theory²⁸⁾ and the reference state of the ΔG_{a}^0 in the present case is $\theta=0$ at the interface. Then, the s_{Li}^w is expressed as

$$s_{\text{Li}}^w = b_{\text{Li}}^w \exp\left(\frac{-F}{RT} \varphi_2^w\right), \quad (8)$$

where

$$\varphi_2^w = -\frac{2RT}{F} \sinh^{-1}(pq^w),$$

and

$$p = (8RT \times 10^3 \varepsilon^w b_{\text{Li}}^w)^{-1/2}.$$

In Eq. 8, b_{Li}^w is the concentration of Li⁺ in the bulk of the aqueous phase in mol dm⁻³, φ_2^w the potential at the OHP^w, and ε^w the permittivity in the aqueous phase. Substituting Eq. 8 into Eq. 7, we obtain

$$\begin{aligned} \Delta G_{\text{a,total}}^0 - \Delta G_{\text{a,f}}^0 = \\ -RT \ln[1 + K b_{\text{Li}}^w (pq^w + \sqrt{(pq^w)^2 + 1})^2]. \end{aligned} \quad (9)$$

The solid lines in Fig. 9 are the calculated curves using Eq. 9 for $Kb_{\text{Li}}^w=1, 10, 100$, and 1000, $b_{\text{Li}}^w=0.05$ mol dm⁻³, $\varepsilon^w=78.36$, and $T=298.15$ K. Figure 9 shows that $\Delta G_{\text{a,total}}^0 - \Delta G_{\text{a,f}}^0$ decreases with an increase in q^w , i.e., an increase in E ; Eq. 9 conforms to the observed tendency of C12E4 adsorption. The increase in K gives rise to an enhancement of both $\Delta G_{\text{a,total}}^0 - \Delta G_{\text{a,f}}^0$, at a given q^w and its

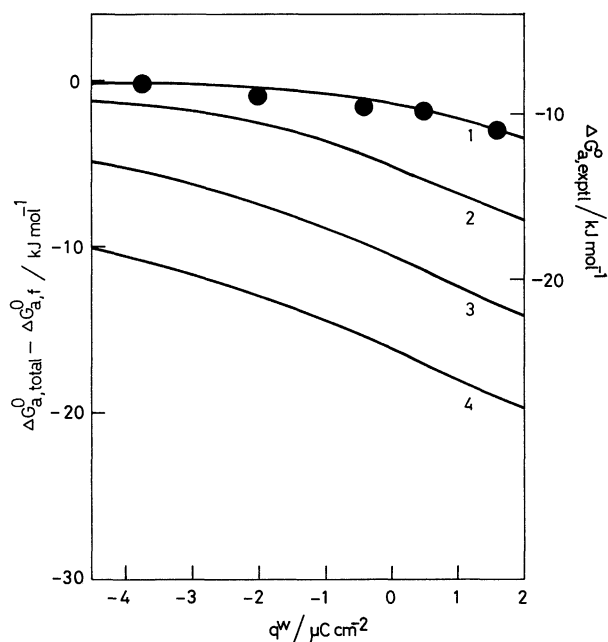


Fig. 9. Dependence of ΔG_a^0 on q^w calculated from Eq. 8 at $K^b c_{Li}^w = 1(1)$, 10(2), 100(3), and 1000(4) at 25 °C when $c_{Li}^w = 0.05 \text{ mol dm}^{-3}$. Filled circles are experimental values.

dependence on q^w . It is interesting to note that the effect of complex formation on ΔG_a^0 is appreciable even in the negative branch, where $q^w < 0$ and the aqueous side of the interface is densely populated with anions, Cl^- , in the present case. The fact that the curvature of the calculated curves in Fig. 9 depends on the K value may be utilized to estimate an experimental K value by fitting the calculated curve to the experimentally obtained ΔG_a^0 vs. q^w curve. The experimental ΔG_a^0 values, $\Delta G_{a,\text{exptl}}^0$, in Fig. 7 are replotted in Fig. 9 as a function of q^w , which was calculated from the electrocapillary curve when $\alpha=0$ (Fig. 8a). The vertical axis was shifted, so that the best fit of experimental points to a calculated curve was obtained, assuming that $\Delta G_{a,f}^0$ is independent of q^w . The best fit of the calculated curve to the experimental one was obtained when $K^b c_{Li}^w = 1$ ($K = 20 \text{ dm}^3 \text{ mole}^{-1}$) and $\Delta G_{a,f}^0 = -8 \text{ kJ mol}^{-1}$. In view of a rather rudimentary stage of the above proposed treatment, it would be premature to discuss physical meanings of these values at any length, though they seem reasonable. Further studies by changing the concentration and the ionic species in the aqueous phase will be desirable to judge the scope of the present model. A further refinement of the present treatment is to incorporate the difference in the energies of the double layer charging as the Frumkin's model, since in the potential range between $E=0.15$ and 0.25 V the difference between the two C_{dl} values is considerable (Fig. 8b). This correction should introduce a quadratic dependence of $\Delta G_{a,\text{total}}^0$ on E through $\Delta G_{a,f}^0$. An estimation of the value of C_{dl} when $\theta=1$ is

necessary for the refinement of the adsorption model along this line.

Another evidence for the surface complexation of C12E4 with Li^+ ions is the shift in the electrocapillary maxima, corresponding to the potential of zero charge, pzc, to the negative potential in the course of the adsorption (Fig. 2). This negative shift can be ascribed to the specific adsorption of Li^+ ions at the interface from the aqueous side, as is the case of the specific adsorption of Li^+ ions to the hydrophilic part of a phosphatidylcholine monolayer.²⁹⁾ The increase in C_{dl} values in the curve 2 in Fig. 8b probably corresponds to this specific adsorption. Since the Li^+ ion, itself, is not specifically adsorbed at the interface in the absence of C12E4 adsorption, the presence of the specific adsorption in the present system indicates that the adsorption of C12E4 induces the specific adsorption of Li^+ ions, which in turn stabilizes the adsorbed C12E4 molecules; the simultaneous adsorption of C12E4 and Li^+ exhibits synergism. This kind of cooperative action has not been reported in the adsorption of nonionic surfactants at mercury–water as well as at air–water interfaces, and can be attributed to the uniqueness of the polarized oil–water interface, where the surfactants and counterions belong to the separate phase and their electrochemical potentials may be controlled independently.¹⁹⁾

Appendix

Experimentally, the standard adsorption Gibbs energy can be obtained from the adsorption coefficient, which can be estimated from either fitting an appropriate theoretical isotherm to an experimental one or the limiting slope of an experimental isotherm when the concentration of adsorbate is infinitely small. The reciprocal plot based on the Langmuir isotherm obviously gives the same quantity. From Eqs. 5 and 6,

$$\frac{d\Gamma_{\text{exptl}}}{dc_{\text{C12E4}}^{\text{NB}}} = (1 + K^s c_{\text{Li}}^w) \frac{d\Gamma_{\text{C12E4}}}{dc_{\text{C12E4}}^{\text{NB}}}$$

and

$$\lim_{c_{\text{C12E4}}^{\text{NB}} \rightarrow 0} \left(\frac{d\Gamma_{\text{exptl}}}{dc_{\text{C12E4}}^{\text{NB}}} \right) = (1 + K^s c_{\text{Li}}^w) \lim_{c_{\text{C12E4}}^{\text{NB}} \rightarrow 0} \left(\frac{d\Gamma_{\text{C12E4}}}{dc_{\text{C12E4}}^{\text{NB}}} \right).$$

Hence,

$$B_{\text{exptl}} = (1 + K^s c_{\text{Li}}^w) B,$$

where B_{exptl} is the experimentally observed adsorption coefficient and B is the corresponding quantity in the absence of the complex formation. Thus,

$$\begin{aligned} \Delta G_{a,\text{exptl}}^0 &= -RT \ln B_{\text{exptl}} \\ &= -RT \ln B - RT \ln (1 + K^s c_{\text{Li}}^w) \\ &= \Delta G_{a,f}^0 - RT \ln (1 + K^s c_{\text{Li}}^w), \end{aligned}$$

which is identical with Eq. 7.

References

- 1) J. Guastalla, "Proc. Second International Congress of Surface Activity III," Butterworths, London (1957), p. 112.
 - 2) A. Watanabe, M. Matsumoto, H. Tamai, and R. Gotoh, *Kolloid Z. Z. Polym.*, **220**, 152(1967); *ibid.*, **221**, 47 (1967).
 - 3) T. Kakiuchi, M. Kobayashi, and M. Senda, *Bull. Chem. Soc. Jpn.*, **60**, 3109 (1987).
 - 4) T. Kakiuchi, M. Kobayashi, and M. Senda, *Bull. Chem. Soc. Jpn.*, **61**, 1545 (1988).
 - 5) M. Senda, T. Kakiuchi, T. Osakai, and T. Kakutani, "The Interface Structure and Electrochemical Processes at the Boundary Between Two Immiscible Liquids," ed by V. E. Kazarinov, Springer-Verlag, Berlin (1987), p. 107.
 - 6) M. Blank and S. Feig, *Science*, **141**, 1173 (1963).
 - 7) M. Dupeyrat and E. Nakache, *J. Colloid Interface Sci.*, **73**, 332 (1980).
 - 8) E. Gileadi, "Electrosorption," ed by E. Gileadi, Plenum Press, New York (1967), Chap. 1.
 - 9) B. B. Damaskin, O. A. Petrii, and V. V. Batrakov, "Adsorption of Organic Compounds on Electrodes," Plenum Press, New York (1971), Chap. 3.
 - 10) T. Sotobayashi, T. Suzuki, and K. Yamada, *Chem. Lett.*, **1976**, 77.
 - 11) S. Yanagida, K. Takahashi, and M. Okahara, *Bull. Chem. Soc. Jpn.*, **50**, 1386 (1977).
 - 12) I. Yoshida, R. Takeshita, K. Ueno, and M. Takagi, *Anal. Sci.*, **2**, 53, 447 (1986).
 - 13) G. P. Brierley, M. Jurkowitz, A. J. Merola, and K. M. Scott, *Arch. Biochem. Biophys.*, **152**, 744 (1972).
 - 14) R. J. Levins, *Anal. Chem.*, **43**, 1045 (1971).
 - 15) Z. Yoshida and S. Kihara, *J. Electroanal. Chem. Interfacial Electrochem.*, **227**, 171 (1987).
 - 16) A part of the present study has been presented at the 34th Annual Meeting on Polarography, Nov. 1988(Chiba); Abstract: T. Kakiuchi, T. Usui, H. Maeda, and M. Senda, *Rev. Polarogr.*, (Kyoto), **34**, 24 (1988).
 - 17) T. Kakiuchi, M. Nakanishi, and M. Senda, *Bull. Chem. Soc. Jpn.*, **61**, 1845 (1988).
 - 18) T. Kakiuchi and M. Senda, in preparation.
 - 19) T. Kakiuchi and M. Senda, *Bull. Chem. Soc. Jpn.*, **56**, 2912 (1983).
 - 20) D. J. Donahue and F. E. Bartell, *J. Phys. Chem.*, **56**, 480 (1952).
 - 21) A. N. Frumkin and B. B. Damaskin, "Modern Aspects of Electrochemistry," ed by J. O' M. Bockris and B. E. Conway, Plenum Press, New York (1964), p. 149.
 - 22) A. N. Frumkin, *Z. Phys.*, **35**, 792 (1926).
 - 23) E. Müller and H.-D. Dörfler, *J. Colloid Interface Sci.*, **83**, 485 (1981).
 - 24) R. G. Barradas and F. M. Kimmerle, *J. Electroanal. Chem. Interfacial Electrochem.*, **11**, 128 (1966).
 - 25) D. Vollhardt, *Kolloid Z. Z. Polym.*, **229**, 61 (1969).
 - 26) G. Gouy, *Compt. Rend.*, **149**, 654 (1910).
 - 27) D. L. Chapman, *Phil. Mag.*, **25**, 475 (1913).
 - 28) T. Kakiuchi and M. Senda, *Bull. Chem. Soc. Jpn.*, **56**, 1753 (1983).
 - 29) T. Kakiuchi, M. Nakanishi, and M. Senda, *Bull. Chem. Soc. Jpn.*, **62**, 403 (1989).
-